

Comparison of properties of CdS thin films grown by two techniques

A.I. Oliva^{*}, R. Castro-Rodríguez, O. Solís-Canto,
Víctor Sosa, P. Quintana, J.L. Peña¹

*Departamento de Física Aplicada, Centro de Investigación y de Estudios Avanzados del IPN Unidad Mérida,
A.P. 73 Cordemex, Mérida 97310, Yucatán, Mexico*

Received 5 March 2002; accepted 6 August 2002

Abstract

Polycrystalline cadmium sulfide (CdS) thin films were deposited on glass substrates by chemical bath deposition (CBD) and close-spaced sublimation (CSS) techniques. The typical deposition temperatures between these techniques are quite different. The CdS thin films deposited by CBD were prepared using two methods of bath agitation: magnetic and ultrasonic agitation. We found that films deposited with ultrasonic agitation presented a cleaner surface with minor presence of contaminants, similar to the obtained for CSS films, as demonstrated by Auger analysis. Properties of the CdS films such as morphology, optical transmission, crystallinity and band gap energy, are discussed in order to compare them in both techniques. We obtain that crystallinity of CdS films depends strongly on the temperature used for deposition. In agreement with several works, films prepared by CBD technique presented a cubic structure, while films grown by CSS technique exhibited an hexagonal symmetry. © 2002 Published by Elsevier Science B.V.

Keywords: Cadmium sulfide; Chemical bath deposition; Close-spaced sublimation; Atomic force microscopy

1. Introduction

Cadmium sulfide (CdS) is a common material used in the formation of solar cells devices based on Cu₂, Cu(In, Ga)Se₂ and CdTe [1–3]. Thin films of CdS used as buffer layer present high electrical resistivity, high band gap energy (E_g) and act as optical window when they are deposited with certain thickness (50–90 nm) as a partner of CdTe. CdS present a high transmittance in the visible and a high reflectance in the infrared

region ($E_g = 2.42$ – 2.45 eV). For solar cells applications, CdS films need to have a suitable conductivity ($>10^{16}$ carriers/cm³), and adequate thickness to allow high transmission and good uniformity to avoid electrical short-circuit effects. Particular properties achieved in films depend on the deposition method and the particular conditions of preparation. CdS thin films can be prepared by chemical, physical and electrochemical methods. Thus, CdS thin films have been deposited by molecular beam epitaxy (MBE) [4,5], metal organic chemical vapor deposition (MOCVD) [6,7], close-spaced sublimation (CSS) [8], chemical bath deposition (CBD) [9,10], electro-deposition [11], successive ionic layer adsorption and reaction (SILAR) [12,13], screen printing [14], pulsed laser ablation [15], RF sputtering [16] and spray

^{*} Corresponding author. Tel.: +52-99-81-2942;
fax: +52-99-81-2917.

E-mail address: oliva@mda.cinvestav.mx (A.I. Oliva).

¹ Present address: CICATA-IPN, Km 14.5, Carretera Tampico-Puerto Industrial Altamira, Altamira 86900, Tamaulipas, Mexico.

pyrolysis [17]. Currently, CBD is one of the low-cost chemical methods, most commonly used to fabricate CdS films for CdTe solar cells with high efficiency [18].

In the CBD technique, CdS thin films are formed by decomposition of thiourea in alkaline solutions of the salts of the corresponding cation. The physical properties of the films depend on different growth parameters such as the bath temperature, the relative concentrations of the reactants in the chemical bath, the pH value [19,20], and the type and surface quality of the substrate [21]. The chemical bath for films growth consists basically of a glass beaker containing the reaction solution and the glass substrate in a separated flask. The temperature of the reactants is typically maintained at 75 °C during growth. Substrates are kept fixed in the hot bath, which usually is spinning with a magnetic stirrer to avoid precipitations.

The substrate–ion interaction during the growth process can be modified if an ultrasonic vibration is applied to the bath. Perturbations with ultrasonic frequencies cause the formation, growth and collapse of bubbles on liquids because of the high temperature and pressure reached in a very short time. Also, ultrasound causes a resonant effect on solids impinging vibrations on them, and for that reason it is used for cleaning. When ultrasonic vibration is applied to promote ion-by-ion heterogeneous growth on the substrate, nucleation on its surface results in a preferential adsorption of cadmium and selenium/sulfur ions, over the rest of sub-products of the chemical reaction.

The influence of physical agents when ultrasonication is applied, was recently investigated by Choi et al. [22]. In their pioneer work they prepared CdS films with a combined action of mechanical agitation and ultrasonication. However, they used cadmium acetate, ammonium acetate, and ammonium hydroxide as reagents for the chemical bath, while in this work, we used different reagents. Choi et al. reported an increment on the film average roughness when the Cd salt concentration in the chemical bath was increased, and an increment on films thickness with deposition time. They found that the values of the average roughness and film thickness were duplicated for films deposited with ultrasonication, respect to films deposited without ultrasonication.

The second method used in this work for CdS films preparation was CSS. It is a fast and low-cost method

to obtain polycrystalline CdS films, with a poor thickness control due to the very fast rate of atoms impinging on the substrate. In this method, CdS source material is evaporated and the vapor species migrate and condense onto a substrate closely located above the source. The range of temperatures used for CSS deposition (600–750 °C) are much higher than the range used in CBD technique (60–90 °C).

In this work we report and compare the stoichiometric, morphological, optical and structural properties of CdS thin films deposited by CBD under magnetic agitation and ultrasonic vibration modalities, and by CSS techniques. We found that the temperature and the ultrasonic vibration used during deposition play important roles on the quality and properties of the CdS films obtained.

2. Experimental procedure

CdS thin films were deposited on glass substrates cleaned with carbon tetrachloride, acetone, and isopropyl alcohol and rinsed with distilled water in each step.

Details of the CBD technique are widely described in the literature [19,23,24]. Briefly, the total volume (110 ml) of the chemical bath, is an aqueous solution containing the following molar concentrations of reactants: 0.02 M cadmium chloride (CdCl_2), 0.5 M potassium hydroxide (KOH), 1.5 M ammonium nitrate (NH_4NO_3), and 0.2 M thiourea ($\text{CS}(\text{NH}_2)_2$) as catalytic reagent. All CBD films were deposited using the same concentration of reagents in the chemical bath. The chemical bath solution was contained into a glass beaker and controlled at 75 °C. The glass substrates were supported by Teflon holders and immersed into the bath. Films deposition starts when thiourea is added. The samples were retired one by one from the bath at different times, being 40 min the major time deposition. The resulting transparent and pale yellow films presented high adherence on substrate and bright surfaces. The CBD technique was applied under two modalities.

- (a) Agitating the hot solution with a magnetic stirrer during deposition. This is a common method used to produce high-quality CdS films, and has been demonstrated to be useful to avoid concentration

gradients [23]. Changes on the angular velocity of the magnetic stirrer has not shown to have important effects on the film properties.

- (b) Applying an ultrasonic vibration to the bath solution instead of magnetic agitation. Here, the chemical bath container and the substrates are immersed into a commercial ultrasonic cleaner (42 kHz).

In both modalities, the temperature of the bath was kept at 75 ± 1 °C by means of a Teflon covered type K thermocouple connected to a home-made temperature controller, based on a CN4421TR-D1 Omega device with a solid state relay.

Films prepared by CSS [25,26] were evaporated in an Edwards E-360 vacuum chamber, evacuated at 10^{-6} Torr with a diffusion pump. The source material was CdS powder 99.99% pure from Balzers, heated by Joule effect into a graphite crucible with a controlled temperature until material sublimates at source temperature (T_f). Vapor species condense on glass substrates heated at substrate temperature (T_s) and located 20 mm above the source. A shutter between crucible and substrate is used to control the time of growth. CdS films were deposited using different values of T_f and T_s . T_f varied from 680 to 760 °C, and T_s lied in the range of 180–550 °C. Deposition time was 5 min for all films prepared by CSS technique.

For imaging, we used an AFM AutoProbe CP in the constant force mode with a high-resolution scanner ($5 \mu\text{m} \times 5 \mu\text{m}$) and a large area scanner ($150 \mu\text{m} \times 150 \mu\text{m}$). Four AFM images of different sites of the surface of each film were obtained, at atmospheric pressure and room temperature, for statistics. Images were analyzed with the Proscan software, calculating the rms-roughness (R_{rms}) value.

Film thickness was determined from compositional depth profiles performed by the Auger electron spectroscopy (AES) technique, in an ESCA/SAM Perkin-Elmer PHI 560 equipment with a double pass cylindrical mirror analyzer at $\sim 2 \times 10^{-9}$ Torr. AES profiles were obtained with an Ar^+ beam with 4 keV and $0.36 \mu\text{A}/\text{cm}^2$, yielding a sputtering rate of about 10 nm/min.

X-ray diffraction (XRD) measurements in the grazing incidence mode with 0.5° of beam inclination were performed, using a monochromatic Cu $K\alpha$ radiation ($\lambda = 1.5418 \text{ \AA}$) and an aperture diaphragm of 0.2° , in

a D5000 Siemens diffractometer. Films were carefully mounted so no misalignment was presented. The scanning step used on the goniometer was 0.01° with a counting time of 10 s. The scattered radiation passed through an arrangement of horizontal slits to the detector. Data were collected sequentially at 2θ angle between 5 and 120° .

Optical absorption measurements were performed with a Jobin-Yvon/Spex H20-VIS spectrophotometer using a tungsten halogen lamp. The incident photon flux was normal to the film surface. The investigated wavelength ranged from 300 to 800 nm. The signal was received and processed with a Data Scan-2 controller coupled to a computer. Optical analysis of films deposited by CBD, was realized after eliminating one of the CdS layers deposited on both faces of the substrate. From here, we determined the band gap energy of the films by the equation

$$\alpha^2 = \frac{1}{d^2} \ln^2 \left[\frac{I_0}{I} \right] = A(E - E_g) \quad (1)$$

where α is the absorption coefficient, d the film thickness, I and I_0 the transmitted and emitted light intensities, respectively, A a constant, and E the light energy.

3. Results and discussion

3.1. Stoichiometry and film thickness measurements

Results of the Auger analysis show that the as-grown CdS films surface grown by the two techniques present clear differences among them. Films grown by CBD with ultrasonic vibration look more cleaner and more transparent than the films grown by CBD with magnetic agitation. Chloride, carbon and oxygen appears as contaminants. By the other hand, CSS films looks more opaque than CBD films because of the higher thickness obtained by the major rate deposition, and the major grain size. Results of the Auger analysis on film surfaces are presented in Fig. 1. CBD films deposited with magnetic agitation presented significant signals of chlorine and oxygen, and a high peak of carbon as contaminants. However, the CBD films surface deposited with ultrasonic vibration presented only minor traces of carbon. Clean surfaces were also

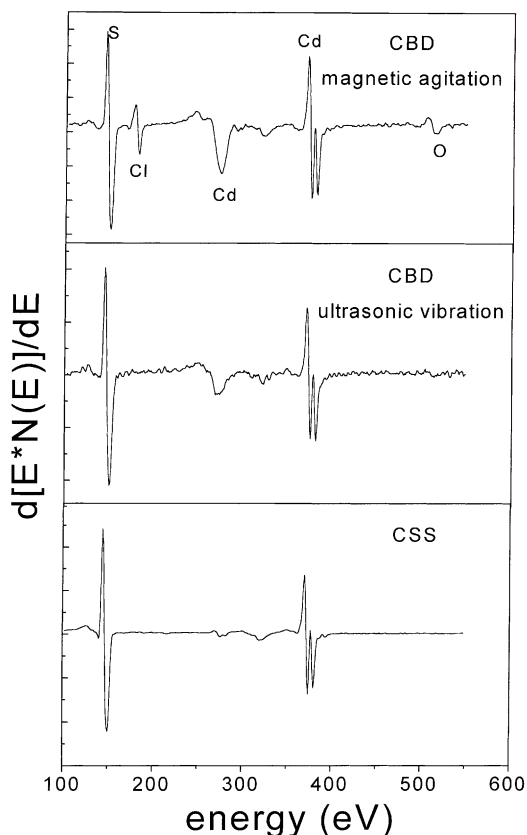


Fig. 1. AES spectra of the samples prepared by the two techniques described in this work. Films with minor contamination were found for CBD with ultrasonic vibration and CSS techniques.

found on CdS films deposited by CSS under vacuum conditions. Therefore, the ultrasonic vibration seems to be a promising CBD modality to diminish surface contamination and improve the surface quality of the

films. This can be explained by the high energy used on the bath solution during ultrasonication, such that colloidal particles are not formed into the bath, reducing the contaminants as a consequence. Similar results have been reported [22] using ultrasonication combined with mechanical agitation for CdS films preparation, obtaining high-quality films without adsorbed CdS particles.

Thickness of samples prepared by CBD with magnetic agitation was 18–20 nm, about five times less than the reported in [22]. Comparatively, thickness of CBD films prepared with ultrasonic vibration and similar deposition times was about 2–3 nm, a minor value than the obtained for films with magnetic agitation. The lower thickness can be due to the ultrasonic action and the magnetic agitation that affects only the bath solution during growth, meanwhile the ultrasonic vibration affects all the system including the substrates.

Comparatively, CSS films were much thicker (0.6–1.0 μm) than CBD films. This was expected, because of the more rapid process of growth due to the major temperature used in this technique.

3.2. Morphological characterization

Fig. 2 shows typical $1\ \mu\text{m} \times 1\ \mu\text{m}$ AFM images of CdS films deposited by CBD during 40 min by the two modalities. Fig. 2a corresponds to films prepared with magnetic agitation. Here, grains appear elongated with a preferential direction. The R_{rms} value measured on image was 9.4 nm. Similar values of roughness have been reported in other works [22,26] for similar conditions. Grains on films deposited with ultrasonic

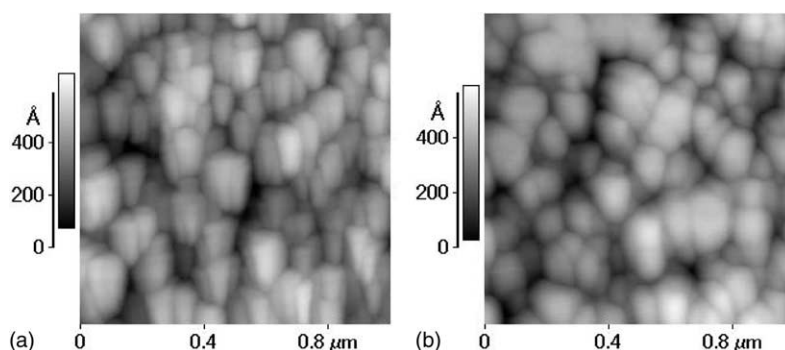


Fig. 2. AFM images of typical CdS films deposited by CBD with: (a) magnetic agitation; (b) ultrasonic vibration.

vibration seem to be more uniform and symmetric than on films prepared by magnetic agitation, as can be observed in Fig. 2b. The R_{rms} value of 9.9 nm found on films prepared by this modality, is closely to the value of the films deposited by magnetic agitation. Grains of films deposited by ultrasonic vibration presented better arrangement; however, given that surfaces are similar to the obtained with magnetic agitation it is difficult to obtain conclusions about them.

Here, it is important to point out that we used for film deposition a constant and low concentration of the Cd reagent (CdCl_2 , 0.004 M) in the chemical bath solution. Maybe, only light differences on the grains shape were found between our CBD films grown by the two modalities. In contrast, Choi et al. [22] reported dramatic morphological changes between film prepared without ultrasonication and with ultrasonication combined with mechanical agitation only when high concentrations of Cd reagent were used (cadmium acetate, 0.008 M). They relate the larger grains observed on films deposited without ultrasoni-

cation with the high concentration of Cd used in the bath. Ultrasonic vibration avoids the formation of colloidal particles, because of the formation of high pressure and hot spots on surface.

Films deposited by CSS method presented a high deposition rate. This is reflected in the high R_{rms} values obtained (about 160 nm). In order to study the influence of the temperature, CdS films were prepared in two groups.

In first group, T_f was ranged from 680 to 760 °C, maintaining T_s at 500 °C. Fig. 3a–c shows 20 $\mu\text{m} \times 20 \mu\text{m}$ AFM images of samples prepared with $T_f = 680$, 720 and 760 °C, respectively. Grains formed with polyhedral geometry and well-defined edges are observed. Clear differences can be seen in the grain size, when T_f increases.

In the second group, T_s was varied from 200 to 550 °C, maintaining T_f at 700 °C. Fig. 3d–f, shows CdS films deposited with $T_s = 200$, 350 and 550 °C, respectively. Changes in the grain size with source temperature can be appreciated. Also, the high source

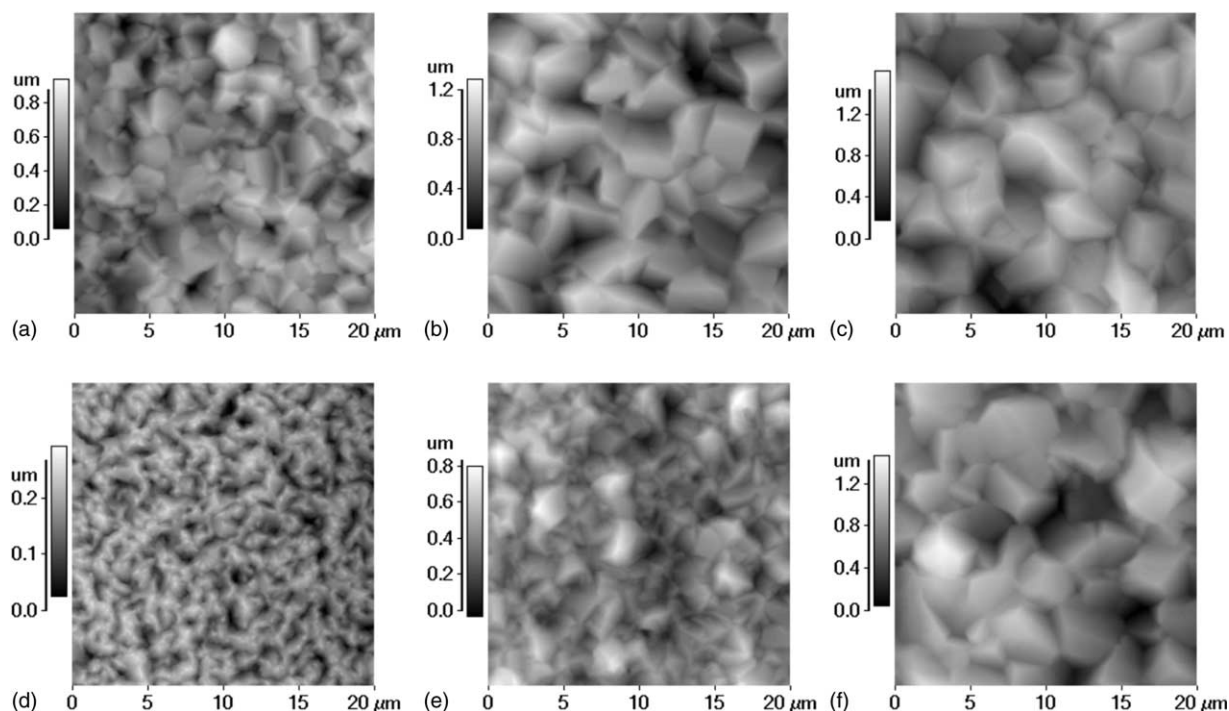


Fig. 3. AFM images of CdS films deposited by CSS at different temperatures. Images (a–c) correspond to samples prepared with constant $T_s = 500$ °C and $T_f = 680$ °C (a), $T_f = 720$ °C (b), and $T_f = 760$ °C (c). Images (d–f) correspond to films grown with constant $T_f = 700$ °C and $T_s = 200$ °C (d), $T_s = 350$ °C (e), and $T_s = 550$ °C (f). The increase of the grain size with temperature is clearly seen in both series.

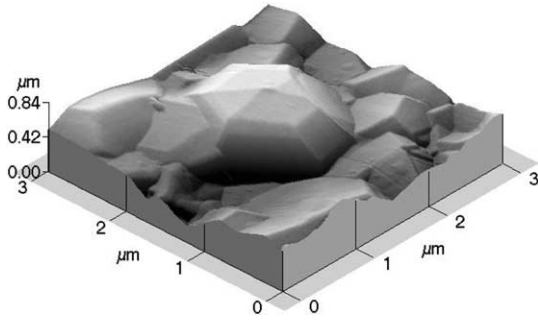


Fig. 4. AFM image of a CdS film grown by CSS ($T_f = 700^\circ\text{C}$, $T_s = 500^\circ\text{C}$), showing a detail of a large and formed grain.

temperature improves the geometry of the grains and their formation. By comparison, Fig. 3c and f seem similar by the high temperatures used for T_f and T_s during deposition, being T_s the parameter of major

influence on the grains formation. Fig. 4 shows a $3\mu\text{m} \times 3\mu\text{m}$ AFM image of a CdS film prepared with $T_f = 700^\circ\text{C}$ and $T_s = 500^\circ\text{C}$ conditions. A $1.5\mu\text{m} \times 1.5\mu\text{m}$ grain with well-defined edges is clearly seen. Similar defined edges but in incomplete grains were observed on films surface grown with $T_f > 650^\circ\text{C}$.

The influence of T_s on surface roughness can be seen in Fig. 5a for CSS films grown at $T_f = 700^\circ\text{C}$. The rms-roughness begins with a low value of 50–100 nm in the range from 300 to 450°C and exhibits an abrupt increment at $T_s > 450^\circ\text{C}$ until to reach a maximum value of 230 nm. The behavior of the surface roughness as T_f changes is shown in Fig. 5b. T_s was maintained constant at 500°C . Here, an asymptotic increment from 130 to 220 nm is observed. Thus, we confirm that T_s has more influence on surface roughness than T_f .

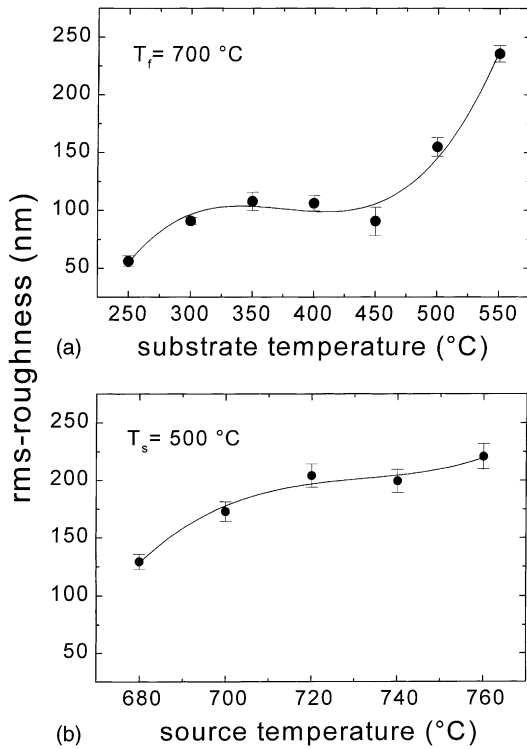


Fig. 5. The R_{rms} values measured on CdS films surface deposited by CSS: (a) as a function of T_s with $T_f = 700^\circ\text{C}$; (b) as a function of T_f with $T_s = 500^\circ\text{C}$. Error bars represent the dispersion of the measurements performed in four different points of each sample.

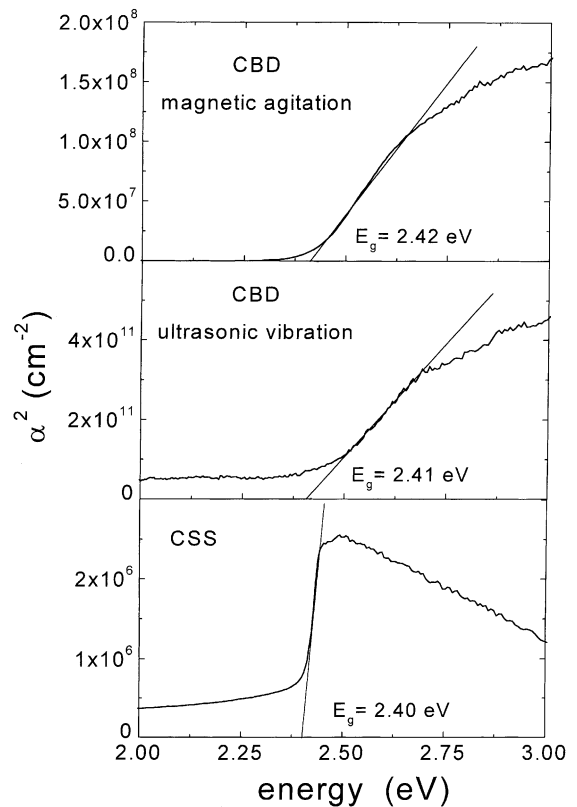


Fig. 6. Energy vs. α^2 curves for typical samples prepared by the two methods. The band gap energy values (E_g) were calculated by a linear extrapolation of the curves to the energy axis.

3.3. Optical characterization

Fig. 6 shows typical curves of the energy versus the squared absorption coefficient for samples prepared by the two techniques. The band gap energy (E_g) was estimated by a linear interpolation of each curve to energy axis, according to Eq. (1). Within an accuracy of ± 0.01 eV, the measured energy gap on films was always in agreement with the reported values (2.4–2.5 eV) for CdS bulk [26–28]. The band gap of CdS films prepared by CBD, both with magnetic agitation and ultrasonic vibration, are shown in the first two curves of Fig. 6. The representative curve of a sample prepared by CSS ($T_s = 500$ °C, $T_f = 700$ °C) is shown in the lower curve of Fig. 6. Note the differences between curves obtained for CBD films and CSS films. Before the absorption band appearing, the optical properties seem similar between films. In CSS films, the slope of the absorption band is more abrupt than the observed on CBD films. Also, in CSS films the curve decays in the high-energy regime (300–400 nm),

indicating a poor filtered effect in this range. Films deposited by CBD do not show this behavior, and present a better filtered property when energy increases. Thus, very thin CdS films with good optical characteristics and clean surfaces can be produced by CBD technique, properly for buffer layer suitable for solar cells application.

Band gap values, measured from samples deposited by CSS are presented as a function of T_s and T_f in Fig. 7. A slight increment of E_g with T_s was obtained (Fig. 7a). A more significant dependence was observed in the band gap values when T_f changed. In fact, for samples deposited at T_f between 680 and 760 °C, E_g was significantly low (Fig. 7b), and a minimum was found at 720 °C. A similar behavior with larger differences was reported by Zelaya-Angel and co-workers [29,30] by photoacoustic spectroscopy technique. They reported a minimum value of E_g attributed to a structural transition from cubic phase to a hexagonal phase when CdS films deposited by CBD were annealed at 300 °C. However, deposition temperatures used in this work are lower (for CBD) and higher (for CSS) than this annealing temperature, depending on the growth technique. We will discuss this result in their relations with temperature with more detail in the next section.

3.4. Structural results

The very small difference (0.021°) between the position of the peak (1 1 1) of the cubic structure and the peak (0 0 2) of the more stable hexagonal structure [27,29] makes difficult to elucidate the crystalline structure [17] of the samples. However, diffractograms registered in a broad range of 2θ (5–120 °C), allowed us to distinguish the two phases. Diffractograms of films prepared by the two techniques are shown in Fig. 8. The films grown by CBD with magnetic agitation and ultrasonic vibration presented cubic symmetry, confirmed by the presence of the peaks (2 2 0) and (3 1 1) associated with this crystallinity. Results previously obtained [31] demonstrate the step-by-step formation of the crystalline structure with time, and after 40 min of deposition, the CdS films show a well-defined cubic structure.

However, as the Fig. 8 shows, all diffractograms for CdS films deposited by CSS under different temperatures always showed the (0 0 2), (1 0 2) (1 0 3),

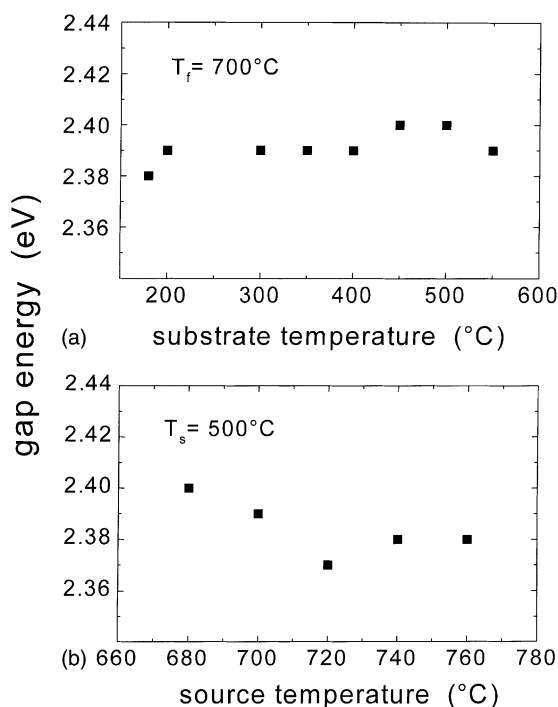


Fig. 7. Band gap energy of CdS films prepared by CSS: (a) as a function of T_s with $T_f = 700$ °C; (b) as a function of T_f with $T_s = 500$ °C. A minimum value of E_g was found at 720 °C.

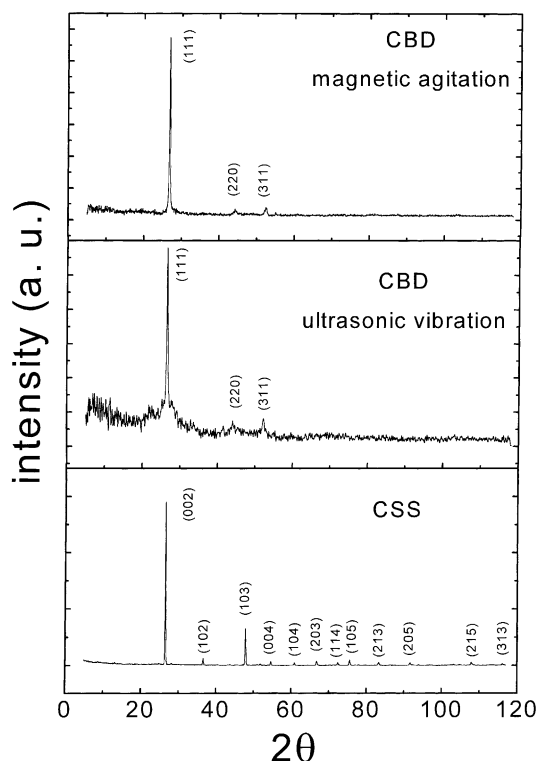


Fig. 8. Typical X-ray diffractograms obtained for films prepared by the two methods. A cubic crystalline structure was found in films grown by CBD, while hexagonal structure was found in samples prepared by CSS.

(0 0 4), (2 0 3), (1 1 4), (1 0 5), (2 1 3) and (2 0 5) diffraction peaks related with the hexagonal CdS phase or Greenockite [32].

Because of that, we suggested that CdS films grown under high temperatures present a high probability of growing with the more stable hexagonal structure.

Several works related with this condition have been published (see [16,33–35]), such as the CdS films prepared on glass substrates by RF sputtering [36] and laser ablation [37]. CdS films prepared at low temperatures (<100 °C), normally show a cubic structure, and films prepared at high temperatures (>300 °C), show hexagonal structures. Also, as-grown CdS samples prepared by CBD [29] or by MBE [38] were reported to have the metastable cubic structure, and a transition to the stable hexagonal phase was found, when films were annealed at 300 °C. In a recent report [30], an analytical study of this phase transformation was discussed. In [22], the authors claimed that

CdS films deposited by CBD on ITO substrates, under ultrasonication, grows only with the hexagonal structure. However, they reported diffractograms which included ITO substrate signals, therefore, their results are not clear at all, except by the formation of the (1 0 1) peak. By the results of our work, and supported by the results of several papers reported on CdS films growth by different techniques, we concluded that the crystalline structure of CdS films depends strongly on the temperature used for preparation. Films produced at low temperatures (as CBD method) will present a major probability for cubic symmetry, while the high temperature used for deposition (as CSS method) or annealing treatments above 300 °C, will result with the stable hexagonal phase. However, the existence of the combined cubic–hexagonal structure obtained on films prepared with techniques or conditions around the transition temperature of 300 °C have been reported. Only a group [39–42], with no clear results of CdS films deposited on glass by the SILAR technique, affirms to obtain a hexagonal structure at room temperature (30 °C) and 80 °C.

4. Conclusions

CdS films were prepared by chemical bath deposition and close-spaced sublimation techniques. For the CBD technique, the bath solution was agitated by two modalities: with magnetic agitation, and with ultrasonic vibration. Agitating by ultrasonic modality, CdS films with low contamination were obtained, similar to the obtained by CSS techniques. In contrast, surfaces of films grown by CBD with magnetic agitation presented contamination by Cl, C and O₂. The ultrasonic vibration results in a low deposition rate of CdS on substrates. The band gap energy values measured in all CdS films, grown by the two techniques, are in good agreement with the typical values reported for the material. The crystalline structure depends strongly on the temperature used during the film deposition or annealing. High temperatures used in the deposition technique (>300 °C) promote the formation of the hexagonal phase, and low temperatures used on the chemical bath deposition technique, produced films with cubic phase crystallinity. However, some of our results are quite different in comparison with other efforts to produce CdS films, with a combined action

of mechanical agitation and ultrasonication on the chemical bath [22] and to study the influence of different deposition techniques [42]. By the other hand, a close approximation for films deposition with vibration effect can be found in [43], where electrical properties of CdS and CdSe films grown by evaporation on vibrating substrates were studied. In that work, authors found that carrier concentration on films decreased with respect to the samples prepared without vibration, whilst the stoichiometry and crystallinity improved.

Acknowledgements

This work was possible by the financial support given by CONACYT, Mexico, through grant 28778-E. Authors thank the technical support given by Pascual Bartolo, Emilio Corona, Wilian Cauich, Roberto Sánchez, Daniel Aguilar, Victor Rejón and Oswaldo Gómez.

References

- [1] T.L. Chu, S.S. Chu, *Solid State Electron.* 38 (1995) 533.
- [2] B. Dimmler, H.W. Schock, *Prog. Photovoltaics Res. Appl.* 4 (1996) 425.
- [3] M.A. Contreras, B. Egaas, K. Ramanathan, J. Hiltner, A. Swartzlander, F. Hasson, R. Noufi, *Prog. Photovoltaics Res. Appl.* 7 (1999) 311.
- [4] G. Brunthaler, M. Lang, A. Forstner, C. Giftge, D. Schikora, S. Ferreira, H. Sitter, K. Lischka, *J. Cryst. Growth* 138 (1994) 559.
- [5] R.P. Vaudo, D.B. Eason, K.A. Bowers, K.J. Gosset, J.W. Cook, J.W. Schetsina, *J. Vac. Sci. Technol. B* 11 (1993) 875.
- [6] H.C. Chou, A. Rohatgi, E.W. Thomas, S. Kamra, A.K. Bhat, *J. Electrochem. Soc.* 142 (1992) 254.
- [7] H.C. Chou, A. Rohatgi, *J. Electron. Mater.* 23 (1994) 31.
- [8] T.L. Chu, J. Britt, C. Ferekides, C. Wang, C.Q. Wu, *IEEE Trans. Electron. Device Lett.* 13 (1992) 303.
- [9] A. Mondal, T.K. Chaudhuri, P. Pramanik, *Sol. Energy Mater.* 7 (1983) 431.
- [10] I. Kaur, D.K. Panda, K.L. Chopra, *J. Electrochem. Soc.* 127 (1988) 943.
- [11] B.M. Basol, E.S. Tseng, D.S. Lo, US Patent 4,548,881 (1985).
- [12] Y.F. Nicolaue, *Appl. Surf. Sci.* 22–23 (1985) 1061.
- [13] Y.F. Nicolaue, M. Dupuy, *J. Electrochem. Soc.* 137 (1990) 2915.
- [14] H. Matsumoto, A. Nakayama, S. Ikegami, Y. Hiori, *Jpn. J. Appl. Phys.* 15 (1980) 129.
- [15] H.S. Kwork, J.P. Zheng, S. Witanachchi, P. Mattocks, L. Shi, Q.Y. Ying, X.W. Wang, D.T. Shaw, *Appl. Phys. Lett.* 52 (1988) 1095.
- [16] S. Bonilla, E.A. Dalchiele, *Thin Solid Films* 204 (1991) 397.
- [17] R.R. Chamberlain, J.S. Skarman, *J. Electrochem. Soc.* 137 (1966) 86.
- [18] J. Britt, C. Ferekides, *Appl. Phys. Lett.* 62 (1993) 2851.
- [19] R. Ortega-Borges, D. Lincot, *J. Electrochem. Soc.* 140 (1993) 3464.
- [20] B.R. Lanning, J.H. Armstrong, *Int. J. Sol. Energy* 12 (1992) 247.
- [21] A.I. Oliva, R. Castro-Rodríguez, O. Ceh, P. Bartolo-Pérez, F. Caballero-Briones, V. Sosa, *Appl. Surf. Sci.* 148 (1999) 42.
- [22] J.Y. Choi, K.J. Kim, J.B. Yoo, D. Kim, *Sol. Energy* 64 (1998) 41.
- [23] J.M. Doña, J. Herrero, *J. Electrochem. Soc.* 144 (1997) 4081.
- [24] J.M. Doña, J. Herrero, *J. Electrochem. Soc.* 144 (1997) 4091.
- [25] J.R. Tuttle, M.A. Contreras, K.R. Ramanathan, S.E. Ashes, R. Bhattachary, T.A. Berens, J. Keane, R. Nonfe, in: *Proceedings of the 44th NREAL/SNL on Photovoltaics Program Review*, 1996, p. 83.
- [26] M. Ichimura, F. Goto, E. Arai, *J. Appl. Phys.* 85 (1999) 7411.
- [27] R. Ramírez-Bonn, N.C. Sandoval-Inda, F.J. Espinosa-Beltrán, M. Sotelo-Lerma, O. Zelaya-Angel, C. Falcony, *J. Phys.: Condens. Matter* 9 (1997) 10051.
- [28] V. Popescu, E.M. Pica, I. Pop, R. Grecu, *Thin Solid Films* 349 (1999) 67.
- [29] O. Zelaya-Angel, J.J. Alvarado-Gil, R. Lozada-Morales, H. Vargas, A. Ferreira da Silva, *Appl. Phys. Lett.* 64 (1994) 291.
- [30] O. Zelaya-Angel, R. Lozada-Morales, *Phys. Rev. B* 62 (2000) 13064.
- [31] A.I. Oliva, O. Solís-Canto, R. Castro-Rodríguez, P. Quintana, *Thin Solid Films* 391 (2001) 28.
- [32] JCPDS, PDF 41-1049 and 10-0454, International Centre for Diffraction Data, PCPDF Win version 1.30, 1997.
- [33] O.A. Ileperuma, C. Vithana, K. Premaratne, S.N. Akuranthilaka, S.M. McGregor, I.M. Dharmadasa, *J. Mater. Sci.: Mater. Electron.* 9 (1998) 367.
- [34] M. Ileva, D. Diminova-Malinovska, B. Rangelov, I. Markov, *J. Phys.: Condens. Matter* 11 (1999) 10025.
- [35] T. Yamada, C. Setiagung, A.W. Jia, M. Kobayashi, A. Yoshikawa, *J. Vac. Sci. Technol. B* 14 (1996) 2371.
- [36] K.E. Assali, M. Boustani, A. Khiara, T. Bakkay, A. Outzourthit, E.L. Ameziane, J.C. Bernade, J. Pouzet, *Phys. State Solid A* 178 (2000) 701.
- [37] H. Sakai, T. Tamaru, T. Sumomogi, H. Ezumi, B. Ullrich, *Jpn. J. Appl. Phys. I* 37 (1998) 4149.
- [38] M. Kobayashi, S. Nakamura, K. Kitamura, H. Umeya, A. Jia, A. Yoshikawa, M. Shimotomai, Y. Kato, K. Takahashi, *J. Vac. Sci. Technol. B* 17 (1999) 2005.
- [39] B.R. Sankapal, R.S. Mane, C.D. Lokhande, *Mater. Res. Bull.* 35 (2000) 177.
- [40] M.P. Valkonen, S. Lindros, M. Leskela, *Appl. Surf. Sci.* 134 (1998) 283.
- [41] C.D. Lokhande, B.R. Sankapal, H.M. Pathan, M. Muller, G. Giersig, H. Tributsch, *Appl. Surf. Sci.* 181 (2001) 277.
- [42] S.A. Al Kuhami, *Vacuum* 51 (1998) 349.
- [43] K.P. Mohanchandra, J. Uchil, *J. Appl. Phys.* 84 (1998) 306.